Polymer 53 (2012) 2255–2264

Contents lists available at SciVerse ScienceDirect

Polymer

journal homepage: www.elsevier.com/locate/polymer

Predicting thermal degradation kinetics of nylon6/feather keratin blends using artificial intelligence techniques

Hakimeh Fazilat [a], Shahin Akhlaghi [a], Mohammad Ebrahim Shiri [b,*], Alireza Sharif [c]

[a] Young Researchers Club, South Tehran Branch, Islamic Azad University, Tehran, Iran
[b] Department of Computer Sciences, Mathematics and Computer Sciences Faculty, Amirkbair University of Technology, Tehran, Iran
[c] Department of Chemical Engineering, Polymer Engineering Group, Tarbiat Modares University, Tehran, Iran

ARTICLE INFO

Article history:
Received 30 November 2011
Received in revised form
5 March 2012
Accepted 25 March 2012
Available online 3 April 2012

Keywords:
Feather keratin
Thermal degradation kinetics
Artificial intelligence techniques

ABSTRACT

A multi-structured architecture of artificial intelligence techniques including artificial neural network (ANN), adaptive-neuro-fuzzy-interference system (ANFIS) and radial basis function (RBF) were developed to predict thermal degradation kinetics (TDK) of nylon6 (NY6)/feather keratin (FK) blend films. By simultaneous implementation of back-propagation ANN and feed-forward ANFIS modeling on the experimental data obtained from thermogravimetric analysis (TGA) method, thermal degradation behavior of various compositions of NY6/FK blends was successfully predicted with minimum mean square errors (MSE). RBF networks were then trained on the TGA data at one heating rate for predicting analogs information at different heating rates, providing sufficient feed for TDK modeling. According to the comparison made between experimental and predicted kinetic parameters of thermal degradation process calculated from Friedman and Kissinger methods, the proposed prediction effort could effectively contribute to the estimation of precise activation energy (E_a) and reaction order (n) values with least amount of experimental work and most accuracy.

1. Introduction

Keratin biopolymer, as the major component of chicken feathers, is constituted of tightly packed polypeptides supercoils cross-linked with disulfide bridges, hydrogen bonds and hydrophobic interactions [1–3]. Such a complex hierarchical structure, particularly when self-assembled in the form of "honeycomb" patterns, makes feather keratin (FK) a highly stable fibrous material with outstanding characteristics [1–3]. Nevertheless, despite chicken feathers are inexpensive and renewable materials available as a waste by-product from poultry plants, reaching millions of tons annually throughout the world, most of feather wastes are commonly disposed by means of landfilling or burning [4–6]. These methods are not merely possessed serious environmental problems, but also waste the opportunity to take full advantage of such promising natural resource [7].

Although, some researchers have pointed out several proposals for developing suitable methods for the application of these bio-organic wastes in value-added areas [8–10], blending FK with other synthetic polymers has attracted much more attention in this regard [11–13]. Indeed, synthetic polymer/FK blends would be more environmental friendly rather than completely synthetic products due to their biodegradation properties provided by FK. Furthermore, these blends would have superior properties compared to the products developed totally from FK.

However, despite the substantial advances made in the fabrication and characterization of the FK containing material, many fundamental aspects have not been satisfactorily discussed in the literature so far, and further investigations are needed to clarify remaining questions in this area. To gain more insight into this issue, in a recent study, we focused on evaluating the miscibility of polyvinyl chloride (PVC)/FK blend films to provide a basic understanding of the interactions between FK and synthetic polymers in both solution and solid states [14]. In another attempt, we also highlighted the thermodynamic surface characteristics of Nylon6 (NY6)/FK blends to attain quantitative information of FK containing blends surfaces at the nanometer scales [15].

Another aspect of FK based blends that has been ignored in the relevant literature is their thermal degradation behavior, which is of great importance in the practical applications of such materials. Since, the kinetic parameters of the thermal decomposition process provide useful information about maximum usable temperature, optimum processing temperature region and life-time of polymer

* Corresponding author. Tel.: +98 2166460948.
E-mail addresses: shahin_723@yahoo.com (S. Akhlaghi), shiri@aut.ac.ir (M.E. Shiri).

0032-3861/$ – see front matter © 2012 Elsevier Ltd. All rights reserved.
doi:10.1016/j.polymer.2012.03.053

materials [16,17], works on thermal degradation kinetics (TDK) analysis can properly elucidate this issue. Although a variety of kinetic models have so far been developed based on thermogravimetric analysis (TGA) data for TDK studies [18,19], the major disadvantage of these approaches is that several experiments are necessary at different heating rates for a complete and accurate degradation investigation which require a large amount of samples, processing time and equipment cost. In addition, in the case of polymer blends, one should also acquire the TDK in the whole composition range of the blend constituents which would impose further experimental runs. Concerning the aforementioned difficulties, we believed that the application of artificial intelligence techniques which recently win great honors for their potential to deal with complex polymeric phenomena without the need for experiments would be the key to solve this problem. Once these methods established, they can significantly reduce the experimental work, costs and time losses required for fundamental experiments.

This paper reports on an outstanding architecture for predicting thermal degradation behavior of various compositions of NY6/FK blends using back-propagation of feed-forward artificial neural networks (ANN) and adaptive network based fuzzy inference system (ANFIS) which were implemented on experimental TGA data under one heating rate. The TGA data at two other different heating rates were also predicted based on radial basis function (RBF) of feed-forward neural network. Eventually, the TDK models were inserted into the driven results to evaluate the kinetic parameters of thermal degradation process which further compared with each other.

2. Experimental

2.1. Materials

NY6 (BS700) with a relative viscosity of 2.7 g/dl and molecular weight of 63,000 g/mol was purchased from BASF Co., Germany. Poultry feather was supplied from Zarbal Company, Amol, Iran. The original source of FK was feather fibers, 3–4 cm in length, which were manually cut from feather shaft and thoroughly washed with ethanol and then dried. Furthermore, formic acid (Merck, Germany) as a solvent was used as received.

2.2. Sample preparation

Solution blending method was utilized to prepare various compositions of NY6/FK blends. At the beginning, each of the blend constituents was dissolved individually in their common solvent, formic acid, to create stock solutions. It should be noted that a homogenous solution of the FK in formic acid was obtained by continuous stirring of the FK/formic acid mixture at 80 ± 2 °C for 4 days. Thereafter, the stock solutions were mixed together using a rotary mechanical mixer, operated at a speed of 1000 rpm for 30 min at 50 °C, in such ratios that various mixtures with 20, 40, 60 and 80 wt% of the FK were obtained. The mixed solutions were then spin cast (2000 rpm for 30 s) onto silicon wafers. Finally, the solvent was removed by evaporation in a vacuum oven at 80 ± 2 °C for 48 h. The resultant NY6/FK blend films, namely NY6/FK 20/80, 40/60, 60/40 and 80/20, were conditioned for at least 72 h at 24 ± 2 °C prior to further experiments.

2.3. Characterization methods

2.3.1. TGA measurements

TGA studies of the samples was carried out using a Polymer Laboratories TGA-PL apparatus at the temperature range of 30–500 °C in a nitrogen inert environment with flowing rate of 30 mL/min and the sample size of 0.6 mg. Conventional constant heating rate measurements were run at 5, 10 and 20 °C/min to cover a wide range of thermal conditions. TGA tests were carried out in aluminum crucibles (5.9 × 4.7 mm) where samples were placed without any previous treatment and experiments were run immediately.

2.3.2. Kinetic models

All the degradation kinetic studies begin with a fundamental rate equation which describes the conversion (α) rate, $d\alpha/dt$, through a temperature-independent function of the conversion, $f(\alpha)$, and a temperature-dependent constant rate of reaction, K, that is [16]:

$$\frac{d\alpha}{dt} = Kf(\alpha) \tag{1}$$

The temperature dependence of the rate constant is expressed in terms of Arrhenius equation as [17]:

$$K = A\exp\left(\frac{-E_a}{RT}\right) \tag{2}$$

where A is a frequency factor corresponding to the incidence of molecular collisions that should be obtained to produce a chemical reaction. In addition, E_a, R and T are the activation energy, the gas constant and the absolute temperature, respectively.

The simplest and most frequently used form of the $f(\alpha)$ assumes that the rate of conversion is proportional to the nth order of the material concentration [16]:

$$f(\alpha) = (1-\alpha)^n \tag{3}$$

where n is the order of reaction. By inserting Eqs. (2) and (3) into Eq. (1), rearranging and taking logarithms, Friedman provided the following expression [18]:

$$\ln\left(\frac{d\alpha}{dt}\right) = \ln A + n\ln(1-\alpha) - \frac{E_a}{RT} \tag{4}$$

For each α value, the plot of $\ln(d\alpha/dt)$ versus T^{-1}, obtained from thermograms recorded at several heating rates, should be a straight line whose slope allows the evaluation of the E_a value. The plot of $\ln(1-\alpha)$ against T^{-1} would also give the n value from the maximum slope of the line.

Another technique used to determine the degradation kinetic parameters is Kissinger method. The rate equation of this method can be expressed as follow [19]:

$$\ln\left(\frac{\beta}{T_{max}^2}\right) = \ln\frac{AR}{E_a} + \ln\left[n(1-\alpha_{max})^{n-1}\right] - \frac{E_a}{RT_{max}} \tag{5}$$

where β, T_{max} and α_{max} are the heating rate of TGA experiments, the temperature and conversion at the maximum conversion rate $(d\alpha/dt)_{max}$, respectively. The slope of the linear plot of $\ln(\beta/T_{max}^2)$ versus $(1/T_{max})$ yields the E_a value and its intercept (I) is [19]:

$$I = \ln\frac{AR}{E_a} + \ln\left[n(1-\alpha_{max})^{n-1}\right] \tag{6}$$

the n value can be then calculated from following equation [19]:

$$n = \frac{(1-\alpha_{max})\left[\exp\left(\frac{-E}{RT_{max}}\right)\right]}{R\left(\frac{d\alpha}{dt}\right)}E_a[\exp(I)] \tag{7}$$

2.3.3. Artificial intelligence techniques

Artificial intelligence is a term that in common usage refers to the ability of a machine to perform the same kind of functions that characterize human thought. Several artificial intelligence techniques such as expert systems, evolutionary algorithms, ANN, fuzzy logic (FL) and ANFIS are progressively employed as alternatives for more classical or conventional techniques to solve complicated practical problems [20].

Inspired by the biological nervous system, ANN approach is a fascinating mathematical tool, which can be used to simulate a wide variety of complex scientific and engineering problems [21–23]. This method has attracted considerable interest due to its ability to provide a convenient solution for predicting, modeling and optimizing non-linear systems. The multilayer feed-forward neural network is the workhorse of the neural network which can be used for both function fitting and pattern recognition problems [24,25]. Our feed-forward ANN model is consisting of two individual branches including RBF networks and back-propagation. RBF network is a special type of feed-forward neural network for application in supervised learning problems including three layers, namely the input layer, the hidden layer and the output layer [26].

Nevertheless, the weakness in the ANN approach is that it does not reveal the nature of relationships among the parameters of the process. To address this deficiency, many attempts were made to combine the fuzzy modeling approach with ANN method so that relationships among the parameters can be explicated [27]. By embedding the fuzzy inference system (FIS) into the framework of adaptive networks, one could obtain the ANFIS architecture, which is the backbone of the present work. This method offers the most suitable way to connect the neural and fuzzy systems, taking advantage from smoothness of the FL interpolation and adaptability of the ANN back-propagation [28].

2.3.3.1. Back-propagation ANN modeling. In the present case, a total of four sets of three-layer neural networks are developed for predicting thermal degradation behavior of NY6/FK blends. To accurately represent complicated relationships among variables, internal parameters need to be adjusted through an optimization or so-called learning algorithm. In supervised learning, examples of inputs and corresponding desired outputs are simultaneously presented to the network, which iteratively self-adjusts to accurately represent as many examples as possible. By providing a network of this type with a set of training data, the network is able to learn and then adjusts the interconnection weights between layers. This process is repeated until the network performs well on the training set and can subsequently be used to classify or predict from previously unseen data output. Nonetheless, the data for training the ANN is needed to be carefully selected, to provide the wide range and well distribution.

Training automatically completes when generalization stops improving, as indicated by an increase in the mean square error of the validation samples. To produce an output, the trained network simply performs function evaluation. In this regard, the function "mapminmax" was used to scale the inputs and targets before training; so that they always fall within a specified range [−1,1].

One of the problems occurring during neural network training is called overfitting; so that the network has memorized the training examples, but it has not learned to generalize to new situations [29]. To balance this problem, data were partitioned to (a) training which used to estimate model parameter, (b) validation that checked the generalization ability of new samples and (c) test for monitoring sets. After the network has learned to solve the material problems, new data from the similar domain can then be predicted.

2.3.3.2. FIS modeling. The FIS has four interconnected segments including fuzzifier, fuzzy rule base, fuzzy inference engine (FIE) and defuzzifier. The fuzzifier transforms crisp input into suitable semantic fuzzy information. The fuzzy rule base stores the rules and knowledge required to solve related problems, describing the relationship between system input and output [30,31]. The FIS is the core of the fuzzy system which simulates thinking and decision-making models of humans via approximate reasoning or fuzzy inference, finding solutions to existing problems [30,31]. The defuzzifier also transforms fuzzy information inferred by the FIS into crisp output [30,31].

The fuzzy rule base is formed by the "if-then" fuzzy rule. This group of fuzzy rules is used to describe the relationship between system input and output. The linguistic fuzzy rule of Sugeno's fuzzy rule is as follow [32]:

$$\begin{aligned}&\text{Rule } l\left(R^l\right):\ \text{If}\left(x_l \text{ is } F_i^l,\ \text{and } x_2 \text{ is } F_2^l \ldots \text{and } x_p \text{ is } F_p^l\right),\\&\text{Then}\left(Y = Y^l = c_0^l + c_1^l\, x_1 + c_2^l x_2 + \ldots\, c_p^l x_p\right)\end{aligned} \tag{8}$$

where F_i^l represents fuzzy set or fuzzy terms associated with the input x_i in the lth rule (R^l), Y^l is the system output due to R^l rule, c_i^l signifies as real-valued parameters of fuzzy number ($i = 1, 2 \ldots, p$) and p is the number of membership functions.

Generally, FIE employs the maximum–minimum operational method for inference. The fuzzy information acquired through inference has to perform defuzzification. The defuzzifier uses the center of gravity to transform fuzzy information into crisp output, y^*, which is expressed as in Eq. (9) [32]:

$$y^* = \frac{\sum_{i=1}^{L} \mu_B(y_i) \cdot y_i}{\sum_{i=1}^{L} \mu_B(y_i)} \tag{9}$$

where L is the quantization levels of the output, y_i is the ith quantization value and $\mu_B(y_i)$ is the membership degree of y_i in the fuzzy set B.

2.3.3.3. ANFIS modeling. For the ANFIS modeling, a set of six-layer ANFIS models were developed. Of great interest is the fact that the purposed model was containing all "and", "or" and "not" rules for each blend sample. In addition, a first-order Takagi-Sugeno-Kang fuzzy approach was used for each of the ANFIS models developed in this study; as this method is computationally more effective than other fuzzy models such as Mamdani and Tsukamoto models [28]. Takagi-Sugeno-Kang neuro-fuzzy systems make use of a mixture of back-propagation to learn the membership functions and least mean square estimation to determine the coefficients of the linear combinations in the rule's conclusions [28].

The hyperbolic tangent sigmoid (TANSIG) and PURELIN functions were utilized as transfer functions in the hidden and output layers. The transfer function in the hidden layer should be non-decreasing and differentiable. The TANSIG transfer function is given as follow [29]:

$$f(w) = \frac{2}{1 + \exp(-2w)} - 1 \tag{10}$$

As each input is applied to the network, the network output compared to the respecting target as the data desired to be reached. To minimize the sum of errors, an objective function (OF) is defined as [29]:

$$\text{OF} = \frac{1}{N} \sum_{i=1}^{N} \left(\frac{|\text{target}_i - \text{output}_i|}{\text{target}_i} \right) \tag{11}$$

where N is the number of data and target is experimental data.

Training of the neural network is done in MATLAB environment, using TRAINGDM function. TRAINGDM is a network training function that updates w and b values in a back-propagation according to Levenberg–Marquardt algorithm (LM). LM is a highly efficient, fast convergence and reliable algorithm in locating the global minimum of the mean square error (MSE) method for solving non-linear optimization problems [28]. It should be noted that the ANN used here was trained until the MSE between the data and network output reduced to 10^{-3}.

The membership function of input and output variables in this study adopts Gaussian2 membership functions which are used for specifying fuzzy sets for the concerned ANFIS models. A hybrid learning algorithm was adopted for training each of the ANFIS models because it has the capability of increasing the speed of the ANFIS's learning process. During training, the value of initial step size is fixed at 0.001; since the value of initial step size does not adversely affect the performance of a trained ANFIS model unless it is too high. Table 1 summarizes the details of various aspects pertaining to the developed ANFIS models. The number of input and output neurons is determined by the nature of the problem.

2.3.3.4. RBF networks. RBF as another type of neural networks is a classification and functional approximation paradigm. RBF have certain advantages over ANNs, including better approximation capabilities, simple network structures and fast learning algorithms [26]. Such networks have an input layer, a single hidden layer of nodes with Gaussian density function and an output layer. They could be employed in any sort of model (linear or non-linear) and any sort of network (single layer or multilayer). The basic function in the hidden layer produces a localized response to the input and typically, uses hidden layer neurones with Gaussian response functions. A typical radial function is the Gaussian which in the case of a scalar input is [33]:

$$Y(x) = \exp\left(-\frac{(x-c)^2}{r^2}\right)$$

where x, c and r are input, center and radius, respectively. The RBF has a maximum of 1 when its input is 0. The output increases, as the distance between w and x decrease. Thus, a radial basis neuron acts as a detector that produces 1 whenever the input x is identical to its weight vector w. Commonly, in an RBF network, the mean and standard deviation of the input vector are used as the cluster center and radius, respectively. Once the center and radius have been computed, the output layer can be nonlinearly mapped using the standard combination technique. It is worth noting to mention that if an RBF network is trained with the same set of data several times, it will produce the same MSE for the test and training data.

Table 1
Details of some important aspects associated with the ANFIS Model for each sample.

Parameter	Specification
Number of input variables	2
Number of output variables	1
Number of network layers	6
Initial step size	0.001
Number of rules	39
ANFIS model type	First-order Takagi-Sugeno-Kang model
Number of training iterations	60
Input membership function type	Gaussian2
Output membership function type	Linear
ANFIS training method	Hybrid (Gradient descent method for the antecedent parameters and least squares estimation method for the consequent parameters)

3. Results and discussion

3.1. Thermal decomposition behavior

Fig. 1 shows the TGA curves of pure NY6 and FK and their different blends at the heating rate of 10 °C/min. Pure FK reveals weight loss in three stages which are appeared as regions with different degradation rates in its TGA curve (see Fig. 1). The first stage in the low temperature ranges is due to the removal of its structural water. On the other hand, the second one, between 250 and 280 °C, is related to the FK helix structure degradation followed by thermal pyrolysis of peptide bridges. The third peak around 300 °C can be attributed to the FK backbone cleavage and final decomposition [35]. In addition, a single step degradation process at 300–450 °C was observed for pure NY6 sample (Fig. 1). Although there is no generally accepted mechanism for the thermal decomposition of NY6, it is believed that the primary polyamide chain scission occurs either at the peptide C(O)-NH or at adjacent bonds, most probably at the NH-CH_2 bond which is relatively the weakest in the aliphatic chain. Hydrolysis, homolytic scission, intra molecular C-H transfer and cis-elimination are all suggested as possible primary chain scission mechanisms [36,37].

Thermal behavior of the NY6/FK blends can be discussed in two distinct temperature regions. In the temperature range below 350 °C, increasing the amount of the NY6 component in the blends increased their thermal stabilities, as inferred from the higher onset degradation temperatures of the NY6-rich blends compared to the FK-rich ones. However, as it can be seen from Fig. 1, such a trend was not followed in temperature range above 350 °C. Actually, in temperatures higher than 350 °C, increasing the FK content of the blends increased their thermal stabilities. It seems that the byproducts of the initial thermal degradation of the blends FK component could contribute to the formation of a char layer on the material surface. Such protective barrier, not merely impeded the heat transfer to the system but also decelerated the escape of volatile small molecules from the NY6 or the remaining FK degradation. Accordingly, as can be seen from Fig. 1 the char yield of the prepared blends increases upon the rise of FK content. Interestingly, this protective mechanism of the FK is similar to nitrogen-containing flame retardants in various systems [38]. This finding runs in harmony with conclusion emerged from the TGA studies of other FK containing blends, as reported elsewhere [14].

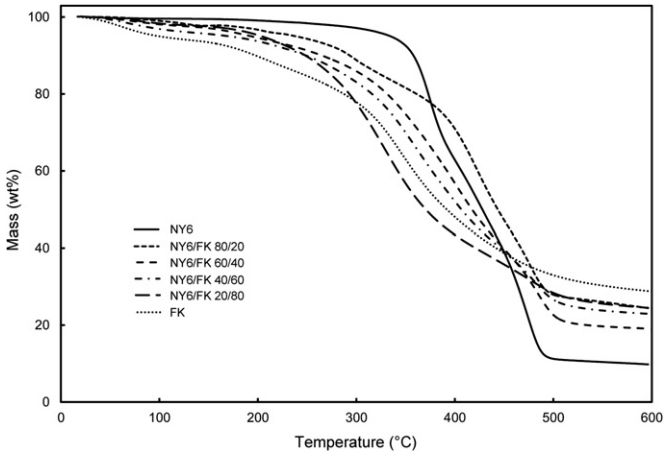

Fig. 1. TGA curves of the pure NY6, FK and their various blends.

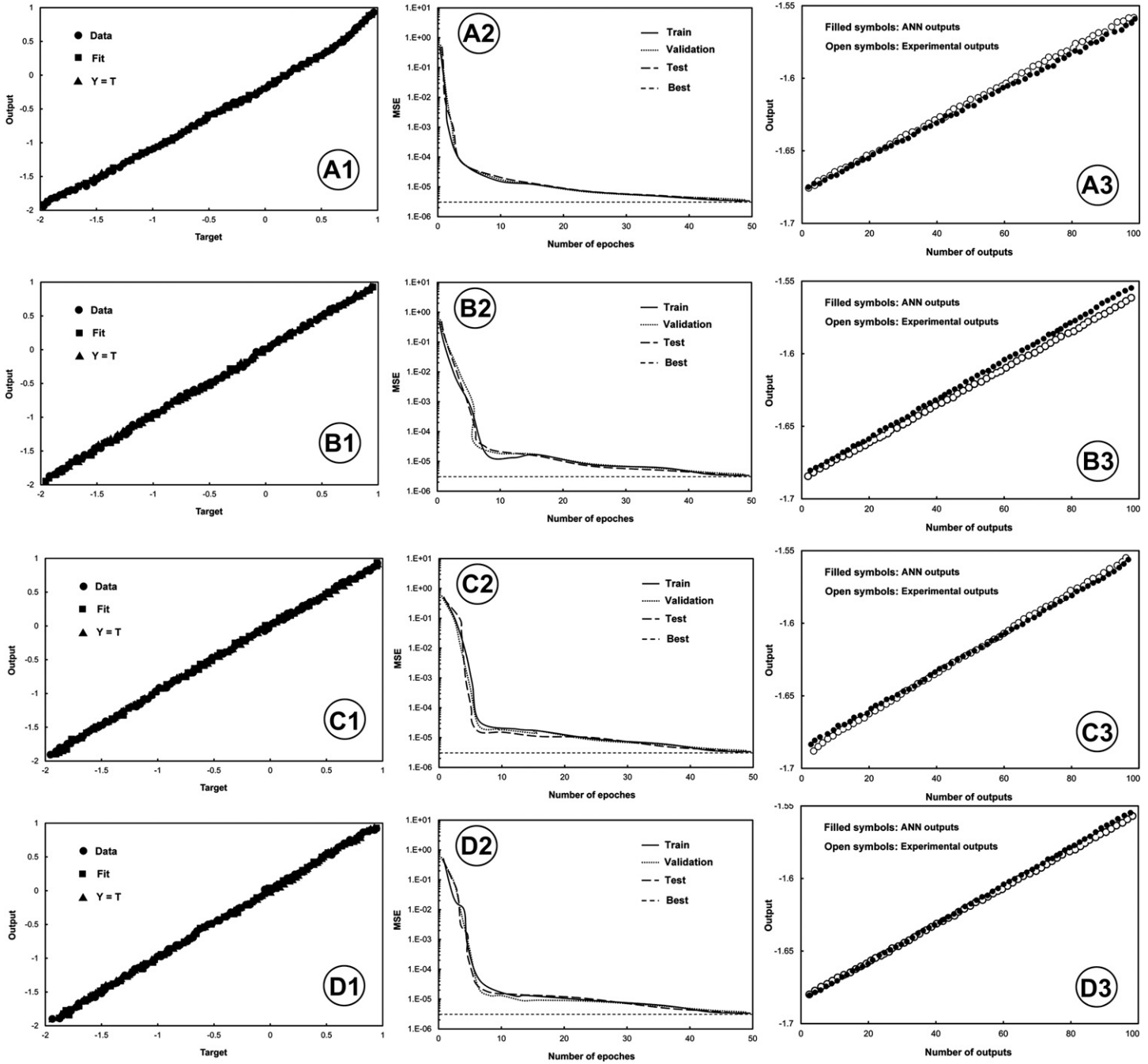

Fig. 2. Regression (1), performance (2) and fitness (3) plots of ANN modeling for NY6/FK 80/20 (A), NY6/FK 60/40 (B), NY6/FK 40/60 (C), and NY6/FK 20/80 (D).

Table 2
Calculated R^2 and RMSE values of ANN modeling for training, validation and testing procedures.

Sample	R^2			RMSE		
	Training	Validation	Testing	Training ($\times 10^{-4}$)	Validation ($\times 10^{-4}$)	Testing ($\times 10^{-4}$)
NY6/FK 80/20	1	1	1	7.6195	8.1735	9.1442
NY6/FK 40/60	1	1	1	181.82	45.242	132.400
NY6/FK 60/40	1	1	1	178.85	60.540	98.678
NY6/FK 20/80	1	1	1	3.8229	3.9696	3.3250

3.2. Prediction of TGA data at various blend compositions

In order to predict the thermal degradation behavior at various compositions of NY6/FK blends, ANFIS approach was applied on the TGA data of pure NY6, FK and their different blend compositions at 10 °C/min. For this purpose, the back-propagation ANN model was preliminary implemented on the TGA data of the entire samples to provide a parameter adaptation for designing neuro-fuzzy systems.

3.2.1. ANN modeling

The ANN models for the studied samples were trained for TGA results with 3168 data sets of which 70%, 15% and 15% of them used for training, testing and validating, respectively. The ANN results including regression, performance and fitness plots for NY6/FK 80/20, 60/40, 40/60 and 20/80 blends are shown in Fig. 2(A–D). The regression plot is used to validate the network performance, perform some analysis of the network response and do a linear regression between the network outputs and the corresponding targets. The regression plots (Fig. 2(A1, B1, C1 and D1)) show the network outputs with respect to targets for training, validation, and test sets. For a perfect fit, the data should fall along a 45° line, where the network outputs are equal to the targets. The correlation coefficient (R^2) value represents normalized measure of the strength of linear relationship between variables which calculated from following expression [34]:

$$R^2 = 1 - \left(\left(\sum_i (t_i - o_i)^2 \right) \Big/ \left(\sum_i (o_i)^2 \right) \right)$$

where t_i and o_i are the target and output values at ith data point, respectively. The higher R^2 values indicate an ANN with better output approximation capabilities. Table 2 shows R^2 values of all data sets for the studied blend samples. It is apparent that the fit is reasonably good for all data sets with R values of 1 for the entire systems (see Table 2). The performance plot of the ANN model is considered as fitness test of the model which shows the MSE values versus the number of epochs to reach the best validation performance for each sample. The quality of the prediction can normally be characterized by root MSE (RMSE) values which are listed in Table 2 for all the blend systems. It was established that the smaller the RMSE of the test data set, the higher is the predictive quality. As can be expected from the nearly zero RMSE values (Table 2), the training and testing data are also reasonably consistent with the validation criteria line for all the studied blend samples (see Fig. 2(A2, B2, C2 and D2)). The fitness plots in Fig. 2(A3, B3, C3 and D3) were used to compare the predicted data (output data) with the experimental ones (target data). The most interesting point is the fact that the predicted results from the training and testing data were remarkably close to each other. From the abovementioned discussions, one can inferred that ANN technique was able to appropriately learn and accurately predict the TGA data of NY6/FK blends.

3.2.2. ANFIS modeling

The ANN modeling results were further combined with FIS rules to provide an ANFIS modeling architecture. Fig. 3 demonstrates the general architecture of driven ANFIS model of two inputs and one output parameters which was implemented for the entire blend samples. Each input was connected to two membership functions

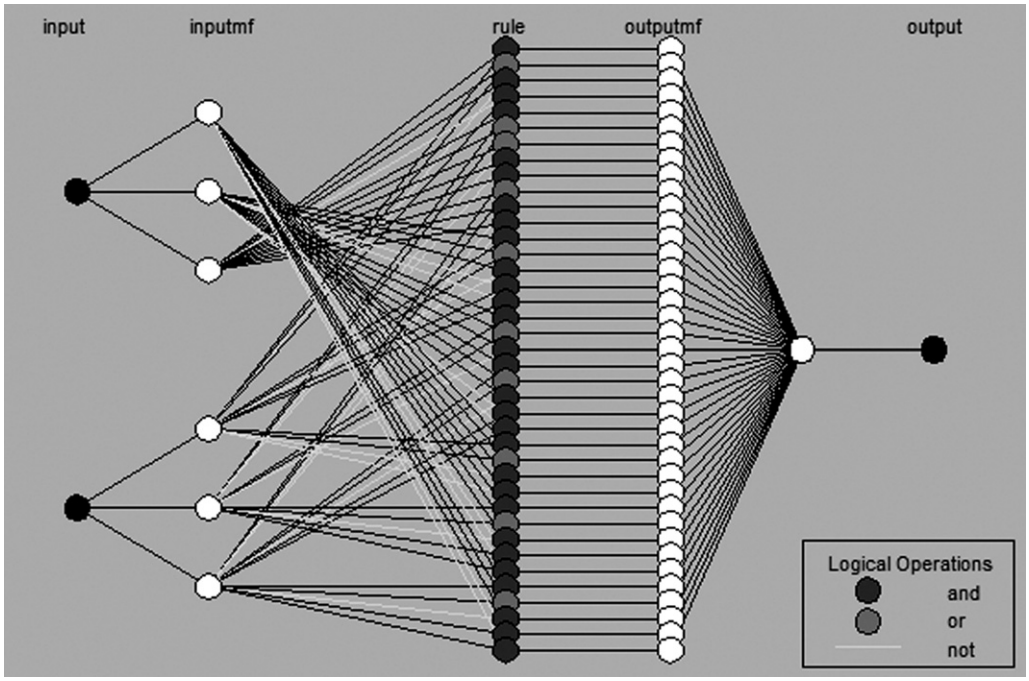

Fig. 3. General architecture of driven ANFIS model for two inputs and one output.

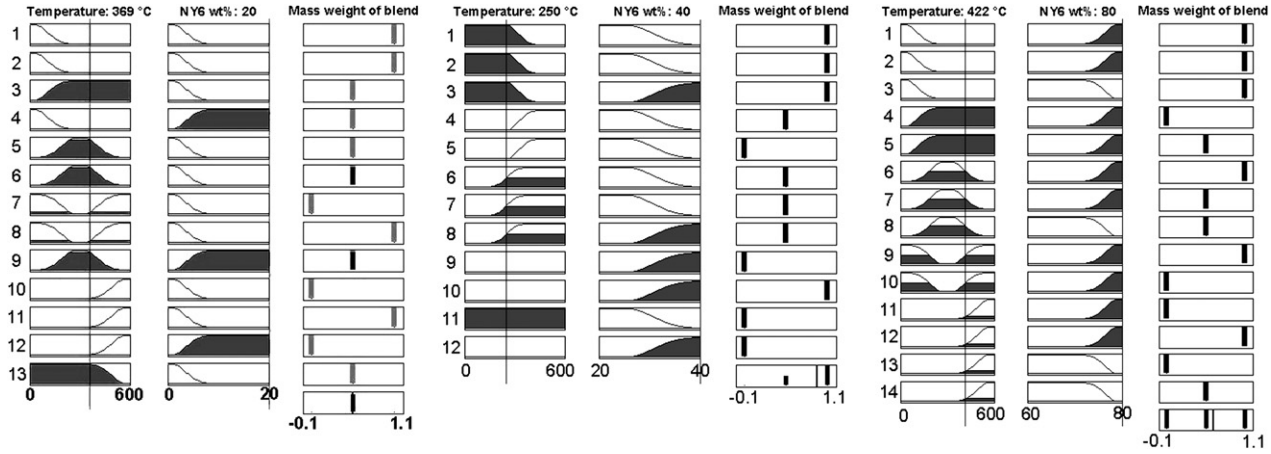

Fig. 4. Rule viewer of NY6/FK 20/80, 40/60 and 80/20 samples at temperatures of 399, 250 and 422 °C.

and further networked with 39 rules. To conclude, these membership functions generated the output. Fig. 4 obviously clarifies the rule viewer of three samples which are selected randomly to show the accuracy of predicted results. Each row in Fig. 4 represents one rule and consists of membership functions corresponding to each of the inputs. The last column is the final output, also identified as consequent membership. As can be seen, the weight loss of the NY6/FK 20/80, 40/60 and 80/20 samples at temperatures of 399, 250 and 422 °C were 0.5, 0.874 and 0.605%, respectively, which are in a good agreement with experimental results.

Fig. 5 shows the surface plot of the predicted TGA data for various NY6/FK compositions. In addition, Fig. 6(A–D) illustrates the output data predicted by ANFIS modeling versus target values of the training and testing for the entire samples. The closeness of the experimental and model-estimated output values clearly points toward the high potential of proposed modeling approach in predicting TGA data at various blend compositions.

To shed more light into the difference between the prediction quality of ANFIS and ANN techniques, the MSE values of predicted data based on both methods were compared for all the blend systems and the results are shown in Table 3. It is clear that the MSE values of ANFIS modeling are lower than that of ANN method. The underlying reason for such observation could be related to the ability of ANFIS to define an inference mechanism that inserts human knowledge about polymer processing into a structured rule basis. Since, the thermal behavior of polymeric systems significantly depend on some sets of particular rules and experimental phenomena, the results obtained from solely ANN modeling could be involved with wide range of unexpectable errors due to the lack of rule viewing. However, concerning the fact that ANFIS modeling produces results based on the fuzzy rules, it might provide more accurate outputs.

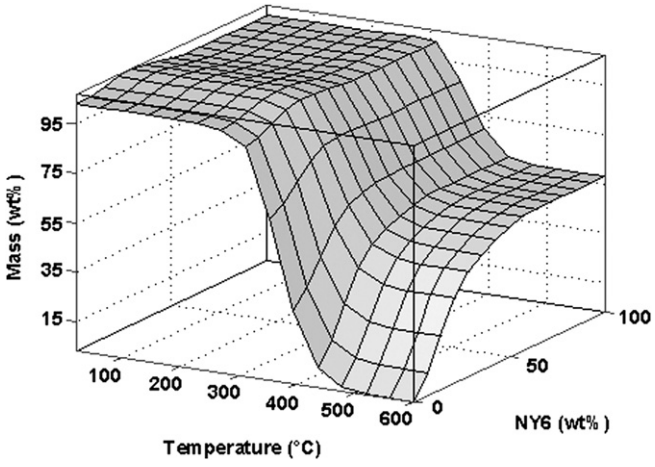

Fig. 5. Surface plot of the predicted TGA data for various NY6/FK compositions.

3.3. Prediction of TGA data at various heating rates

In the view of TDK modeling, TGA data at several heating rates are required to utterly perform the degradation analysis. In this account, RBF model was trained for predicting TGA data at 5 and 20 °C/min based on the experimental results at 10 °C/min. Feed-forward RBF networks perform a specific non-linear input–output mapping by using training data set.

An RBF model with one hidden layer and two inputs including temperature and blend composition was designed. The algorithm was performed using 'newrbf' instructions in MATLAB® software and a Gaussian2 function with 500 data sets. As an example, Fig. 7 illustrates the predicted TGA curve at 5 °C/min in comparison with experimental data at the same heating rate for the NY6/FK 40/60 sample. Interestingly, the predicted data are well coincide with the experimental ones (see Fig. 7).

3.4. TDK analysis

The application of TGA method holds a great promise as a tool for unraveling the kinetic parameters of chemical reactions for the degradation process of material. The TDK of the pure NY6 and FK and their blends based on Friedman and Kissinger techniques are presented here with both experimental and predicted TGA data.

It is possible to obtain the plots of $\ln(d\alpha/dt)$ versus (T^{-1}) and $\ln(l-\alpha)$ versus T^{-1} at different conversions for the entire samples by fitting TGA data at heating rates of 5, 10 and 20 °C/min on Friedman equation (Eq. (4)). For instance, Fig. 8(A and B) illustrates $\ln(d\alpha/dt)$ vs. $(1000/T)$ and $\ln(l-\alpha)$ vs. 1000/T plots of experimental data at α values of 0.2, 0.4, 0.6 and 0.8 in NY6/FK 60/40 blend. According to the thermal decomposition analyses presented in the previous section, the studied samples was clearly shown multi-degradation profiles, meaning the occurrence of plural degradation reactions. Therefore, the lack of parallelity between the fitting straight lines in Fig. 8 is anticipated. On the contrary, it is apparent that the data-points are well fitted to the straight lines ($R^2 > 0.98$) which

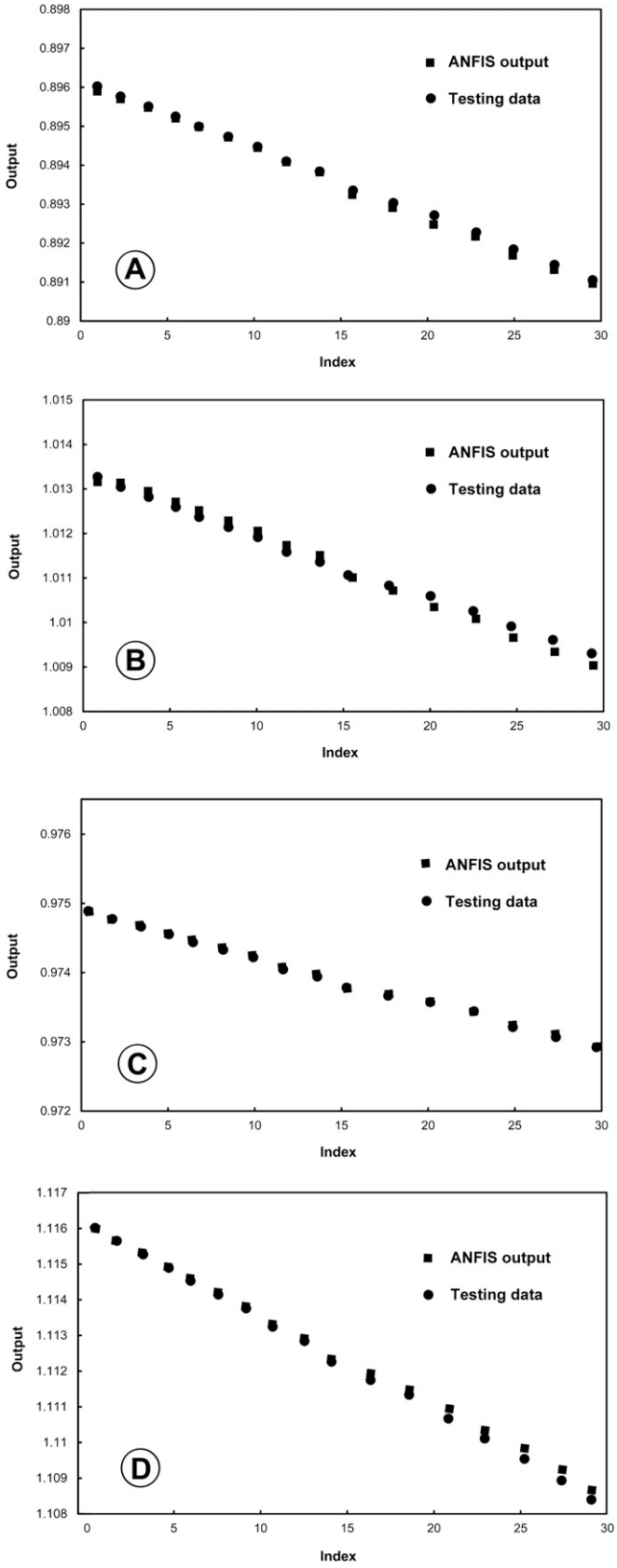

Fig. 6. Comparison between testing data and ANFIS outputs for 80/20 (A), 40/60 (B), 60/40 (C) and 20/80 (D).

Table 3
Comparison between MSE values of ANFIS and ANN methods.

Sample	MSE	
	ANN	ANFIS
NY6/FK 80/20	0.005	0.002
NY6/FK 40/60	0.012	0.006
NY6/FK 60/40	0.011	0.004
NY6/FK 20/80	0.008	0.002

confirms the applicability of Friedman method to study the degradation kinetics of NY6/FK systems In addition, the $\ln(\beta/T_{max}^2)$ versus $(1000/T_{max})$ plots were attained from the application Kissinger model (Eq. (5)) on experimental TGA data. A representative Kissinger plot for experimental TGA data of NY6/FK 60/40 sample is shown in Fig. 9. Reasonable straight lines were obtained for the entire range of experiments.

The E_a and n as average values of kinetic parameters of the entire degradation steps for all compositions were obtained employing both Friedman and Kissinger plots based on the procedure discussed earlier and the results are listed in Table 4. Obviously, the kinetic parameters calculated by both methods did not show any significant difference. One must note however, a slight disagreement between the results obtained from Friedman and Kissinger models might be attributed to different mathematical approaches used to calculate the parameters.

Since E_a can be defined as the minimum amount of energy required to initiate the degradation process, one can consider E_a as a quantitative parameter to compare the initial thermal degradation behavior of materials. The most interesting point concerning the calculated kinetic data was the fact that a tendency to increase in E_a value was observed with increase of NY6 content (see Table 3). This observation is in accordance with our previous finding that the NY6-rich blends had higher degradation onset temperature as compared with FK-rich ones. However, this was not the case for n parameters so that the calculated values were in the order: NY6 > NY6/FK 80/20 > NY6/FK 60/40 > NY6/FK 40/60 > NY6/FK 20/80 > FK. Bearing in mind that the n value is directly related to the consumption rate of the reactants in degradation reaction, such a kinetic parameter could provide a precise insight into the degradation period of the materials. Actually, the decomposition process of sample with lower n value is slower than the one with higher n value. Therefore, one can conclude that the increase of the FK content suppresses the thermal degradation rate of NY6/FK systems.

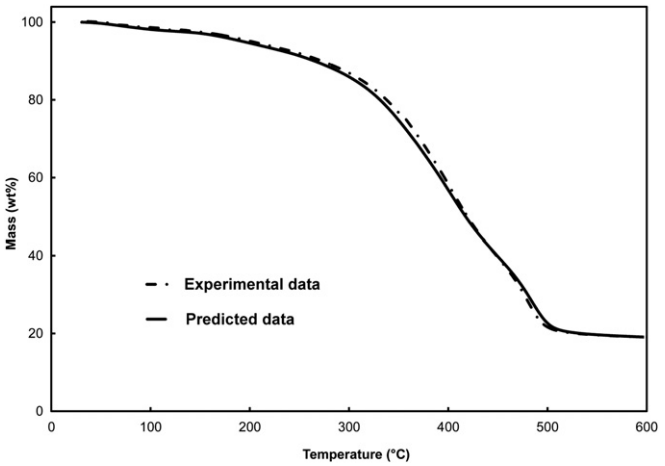

Fig. 7. Predicted TGA curve of NY6/FK 40/60 at 5 °C/min obtained from RBF modeling compared to the corresponding experimental data.

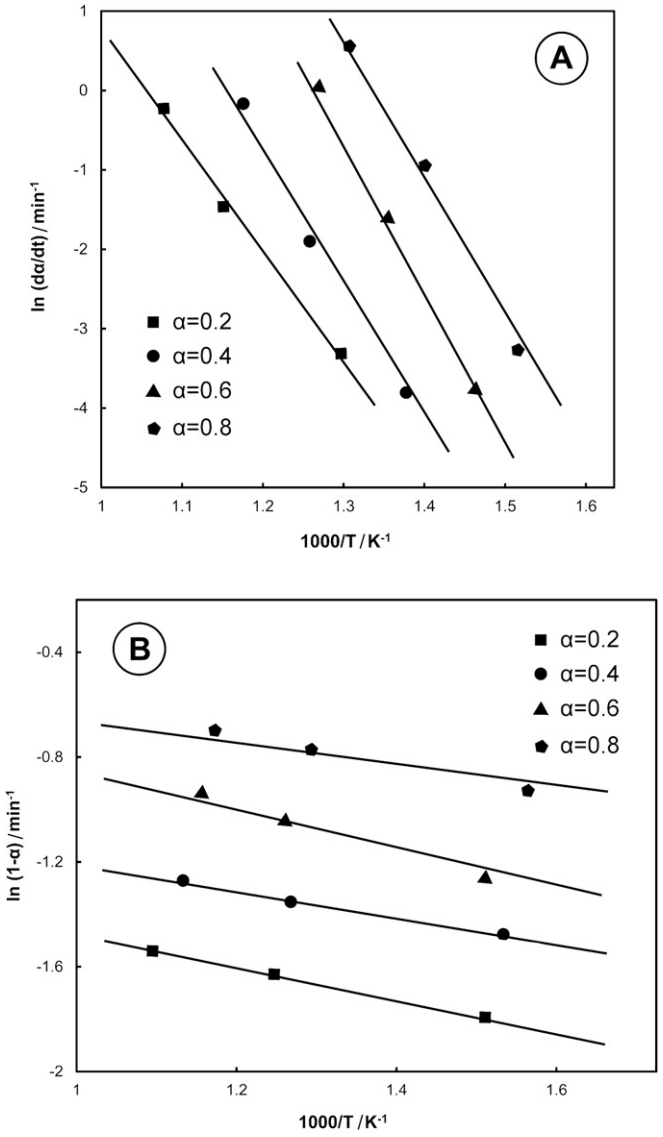

Fig. 8. Friedman graphs for NY6/FK 60/40 sample.

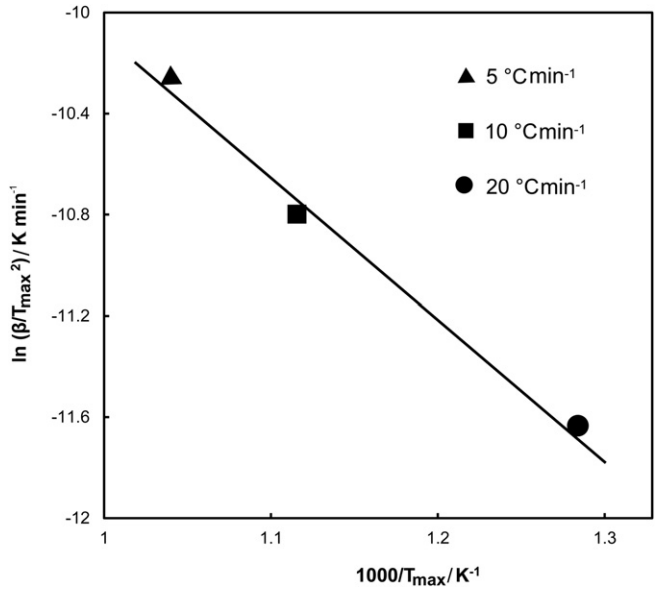

Fig. 9. Kissinger graph for NY6/FK 60/40 sample.

Table 4
The experimental and predicted Friedman and Kissinger E_a and n values of pure NY6 and FK as well as their studied blends.

Sample		Friedman		Kissinger	
		E_a (KJ/mol)	n	E_a (KJ/mol)	n
NY6	Experimental	165	2.01	161	1.97
	Predicted	167	1.98	162	1.95
NY6/FK 40/60	Experimental	129	1.02	137	1.11
	Predicted	130	0.99	140	1.09
NY6/FK 60/40	Experimental	76	0.83	77	0.85
	Predicted	79	0.80	81	0.83
NY6/FK 20/80	Experimental	71	0.79	73	0.82
	Predicted	73	0.77	76	0.82
NY6/FK 80/20	Experimental	68	0.71	69	0.80
	Predicted	66	0.69	67	0.77
FK	Experimental	59	0.65	62	0.75

Similarly, the analytical procedures were preformed on the predicted TGA data for the entire samples (plots not shown here) and the corresponding kinetic parameters are listed in Table 4. Interestingly, the theoretical and experimental E_a and n parameters were found to exhibit not only same trend but also almost analogous values. Accordingly, this finding lend credence to the hypothesis that TDK anlaysis could be carried out by only few amount of experimental data using artificial intelligence techniques.

4. Conclusion

This study set out to predict the thermal degradation kinetics of NY6/FK blend films using several supplementary artificial intelligence techniques namely ANN, ANFIS and RBF. Besides providing experimental data for the prediction modeling, TGA experiments also revealed that the keratinous structure of FK wastes could exhibit a protective mechanism in analogy to nitrogen-containing flame retardant for the studied blends. The thermal degradation behavior of four different compositions of NY6/FK blends was learned by ANN and further predicted by ANFIS in a reasonable agreement with experimental results. By training RBF networks on the TGA data of blend systems at heating rate of 10 °C/min, thermal degradation curves at 5 and 20 °C/min were successfully predicted with the least R^2 and MSE values for the entire samples. TDK analyses were then performed on both the experimental and predicted TGA data using Friedman and Kissinger techniques. The closeness of E_a and n average values obtained from the proposed modeling approach with their experimental counterparts was suggestive of the fact that artificial intelligence techniques could be employed quite effectively for predicting kinetic parameters of thermal degradation process of polymer mixtures particularly NY6/FK blends.

References

[1] Barone JR, Dangaran K, Schmidt WF. J Agric Food Chem 2006;54:5393–9.
[2] Fraser RDB, Parry DAD. J Struct Biol 2008;162:1–13.
[3] Katoha K, Tanabe T, Yamauchi K. Biomaterials 2004;25:4255–62.
[4] Huda Sh, Yang Y. J Polym Environ 2009;17:131–42.
[5] Bertsch A, Coello N. Bioresour Technol 2005;96:1703–8.
[6] Poopathi S, Abidha S. Biol Control 2007;43:9–55.
[7] Poopathi S, Abidha S. Int Biodeterior Biodegrad 2008;62:479–82.
[8] Fujii T, Li D. J Biol Macromol 2008;8:48–55.
[9] Schrooyen PMM, Dijkstra PJ, Oberthur RC, Bantjes A, Feijen J. J Agric Food Chem 2001;49:221–30.
[10] Tanabe T, Okitsu N, Yamauchi K. J Mater Sci Eng C 2004;24:441–6.
[11] Cheng S, Lau K, Liu T, Zhao Y, Lam P, Yin Y. J Composites B 2009;40:650–4.
[12] Barone JR. J Polym Environ 2009;17:143–51.
[13] Sh Huda, Yang Y. J Compos Sci Technol 2008;68:790–8.
[14] Akhlaghi Sh, Sharif A, Kalaee M, Manafi M. J Appl Polym Sci 2011;121:3252–62.

[15] Akhlaghi Sh, Sharif A, Kalaee M, Nouri A, Manafi M. Polym Int 2012;61:646–56.
[16] Paik P, Kar KK. J Polym Deg Stab 2008;93:24–35.
[17] Li XG, Huang MR. J Appl Polym Sci 1999;71:1923–31.
[18] Friedman HL. J Appl Polym Sci 1964;6:183–95.
[19] Kissinger HE. J Anal Chem 1957;29:1702–6.
[20] Abraham AJ. Stud Fuzz 2005;181:53–83.
[21] Chun MS, Biglou J, Lenard JG, Kim JG. J Mater Process Technol 1999;86:245–51.
[22] Bahrami A, Mousavi Anijdan SH, Madaah Hosseini HR, Shafyei A, Narimani R. J Comput Mater Sci 2005;34:335–41.
[23] Kim DJ, Kim BM. J Mach Tools Manuf 2000;40:911–25.
[24] Hinton GE. J Artif Intelligence 1989;40:185–234.
[25] Hinton GE. J Scientific Am 1992;267:144–51.
[26] Chen S, Cowan CNF, Grant PM. IEEE Trans Neural Networks 1991;2:302–9.
[27] Zadeh LA. Inf Control 1965;8:338–53.
[28] Ubeyli ED, Guler I. Neurocomputing 2006;70:296–304.
[29] Sedighi M, Keyvanloo K, Towfighi. J. Ind Eng Chem Res 2011;50:3–10.
[30] Bose S, Shome D, Das CK. Arch Comput Mater Sci Surf Eng 2009;1:197–204.
[31] Zhou Q. Energy Procedia 2011;4:2066–73.
[32] Hsiang SH, Lin YW. The Arab J Sci Eng 2009;34:175–85.
[33] Bishop C. Neural Comput 1991;3:579–88.
[34] Karaman S, Kayacier A. LWT - Food Sci Technol 2011;44:1717–25.
[35] Verbeek CJR, Van Den Berg LE. J Macromol Mater Eng 2010;295:10.
[36] Holland Barry J, Hay James N. J Polym Int 2000;49:943–8.
[37] Levchik Sergei V, Weil Edward D, Lewin Menachem. J Polym Int 1999;48:532–57.
[38] Lu S, Hamerton I. J Prog Polym Sci 2002;27:1661.